IEEE Access
Multidisciplinary | Rapid Review | Open Access Journal

Received November 24, 2021, accepted December 9, 2021, date of publication December 22, 2021, date of current version January 5, 2022.

Digital Object Identifier 10.1109/ACCESS.2021.3137324

A Beam-Split Metasurface Antenna for 5G Applications

TAMARA Z. FADHIL[1,2], NOOR ASNIZA MURAD[1], (Senior Member, IEEE), MOHAMAD KAMAL A. RAHIM[1], (Senior Member, IEEE), M. R. HAMID[1], AND LEVY OLIVIA NUR[3], (Member, IEEE)

[1]Advanced RF and Microwave Research Group (ARFMRG), Faculty of Engineering, School of Electrical Engineering, Universiti Teknologi Malaysia (UTM), Johor 81310, Malaysia
[2]College of Engineering, University of Information Technology and Communications, Baghdad 10013, Iraq
[3]Fakultas Teknik Elektro, Universitas Telkom, Bandung 40257, Indonesia

Corresponding author: Tamara Z. Fadhil (tamara@graduate.utm.my; tamara.zuhair@uoitc.edu.iq)

This work was supported in part by the Ministry of Higher Education (MOHE), School of Postgraduate Studies (SPS), Research Management Centre, Advanced RF and Microwave Research Group, School of Electrical Engineering, Universiti Teknologi Malaysia (UTM), Johor Bahru, under Grant 4B590, Grant 5F423, Grant 21H69, and Grant 09G19.

ABSTRACT This article presents a hybrid metasurface split beam antenna for fifth-generation (5G) mobile applications at 3.5 GHz. Multi-beam antennas with high directivity are required for a 5G mobile network. It can be achieved by having an array antenna. Using an antenna array at low frequency increases the complexity and size of the whole network. Therefore, a metasurface (MS) is proposed to direct surface current and to have high gain and multibeam properties. To achieve that, a square split ring resonator (SSRR) and U-shaped unit cell metasurface is implemented as a superstrate to a single square patch antenna. The manipulation of this hybrid metasurface configuration can create opposite current flow on the unit cell and thus split the beam. The hybrid metasurface superstrate and antenna are fabricated on FR-4 ($\varepsilon r = 4.4$, $\tan\delta = 0.02$). Results show that the antenna resonates well at 3.5 GHz, with a less than -10 dB reflection coefficient. The arrangement of the unit cells on the superstrate metasurface is able to split the current, and thus the radiation pattern beam is split into two beams in the E-plane at $\pm$ 45°. This antenna is a good candidate for future 5G Pico cell base stations in urban or suburban areas with high capacity and interferences.

INDEX TERMS 5G, beam split, metasurface, SSRR.

I. INTRODUCTION

Currently, the rapid growth of wireless communication demands for higher capacity and greater speed pushed the swift growth of telecommunication systems to the next generation. The fifth-generation (5G) is introduced to support demands with higher throughput. A higher gain antenna is needed, and thus array structures were suggested in many research to have a higher gain performance system with the ability to switch the beam and avoid interferences. Antenna array and multi-beam antennas are widely used in the wireless communications field where 5G base stations are integrated with multiple antennas that would be compatible for high capacity, high gain, and high efficiency [1]–[3]. Specifically, antenna array and multi-beam antennas increase the capacity and cover a broader range of locations, which leads to improving the whole base station systems [4].

Additionally, enhancing the infrastructure cost reduces the total cost of the 5G base stations. Hence, these advantages will be particularly welcoming in the future of lower band 5G applications [5].

The fifth-generation (5G) systems are required to provide multiple beams with high gain and capacity towards the target. Hence, 5G technology suggests a lower band of 3.5 GHz for 5G mobile applications [6]. However, at this frequency of 3.5 GHz, the antenna array is quite big and inflexible. Therefore, Metamaterial structures are proposed for having a compact, miniaturized wideband antenna, reshaping radiation patterns and steering multiple beams [4]–[7].

Metamaterials are artificially magnetic materials (AMMs) structured to demonstrate electromagnetic properties that are impossible to achieve with ordinary materials at desired frequencies [8]. AMM is one of the contemporary materials,

The associate editor coordinating the review of this manuscript and approving it for publication was Yang Yang.

consisting of metal structures arranged on the interface of dielectric substrates. As a result, metamaterials' physical qualities depend more on their structures than on the components that make them up [9], [10]. In 1968, Veselago was the first expert who contributed to developing the metamaterials' structures by characterizing the essential parameters, permittivity (ε), and permeability (μ) [11], [12].

The split-ring resonator (SRR) is one of the metamaterials' most essential tiny components for obtaining artificial magnetism at microwave frequencies [13].

A compact of two-dimensional metamaterials (unit cells) construct a metasurface (MS) which are optically thin subwavelength resonators [14]. By using metamaterial and metasurface implementation on the feed lines, patch lines, as superstrate and background of the microstrip substrate, increases the bandwidth, gain, and directivity and reduces the antenna size. Hence, that will bring additional functionality by meeting the requirements of the communication devices for 5G applications.

Recently, the metasurface-based antenna is in interest due to its low profile, compact size, and its ability to produce multiple beams in various directions [15].

In terms of metasurface performance, as explained previously in [16], the metasurfaces can be configured for near-field modification for gain optimization. This type of technology (near-field transformation) has also been used to reshape radiation patterns, as discussed in [17]. Another current method exhibiting improving gain, a monopole antenna with wideband was developed using a double split ring metasurface [18].

The metasurface is widely used in antenna design to enhance the gain, bandwidth, polarization, and steering of the antenna beams [19]–[23]. It has the capability to steer beams or produce multiple beams antennas with high gain and polarization characteristics [24], [25]. However, it has a drawback of large size and uses antenna array as a source of multiple beams [26]–[28]. This is mainly due to the air gap between the metasurface and the radiating antenna [29], [30]. For example, the metasurface in [24] has good beam steering characteristics but it's a narrow beam scanning due to the antenna beam characteristics which makes it not possible to be used in the 5G band. Thus, a metasurface that could split and steer the beam in multiple directions is needed for the 5G mobile application.

Several recent research on metasurface antennas to control and split the antenna beams have been done. As in [31], digital coding metasurface is used to split an antenna beam. However, this technique depends on digital coding for only splitting one beam into two beams with considerable sidelobes. Upgrading this technique to more than two beams results in very complex coding and structure. Besides, PIN diodes-based reconfigurable metasurface antenna are presented for beam switching applications and split beam with dual operations depends on the diode bias states [32], [33]. The suggested antenna results exhibit good impedance matching and slight gain performance over the frequency range. The major drawback of these approaches is developing a reconfigurable metasurface as demonstrated involves a large number of PIN diodes. In [34], a reshaping multibeam is proposed by an arrangement coding in a metasurface. Flexible phase responses are acquired by inserting a varactor into all unit cells. Although the outcomes of the experiments confirm the performance of the design technique, this approach might not be convenient for some drawbacks. Such as; considerable metasurface with super unit cells covering a 300×300 mm^2 area ($5.6\,\lambda_0 \times 5.6\,\lambda_0$). In addition, to achieve three beams, the energy of the two beams in the center is missing compared to the three beams.

On the other hand, a linear metamaterial is concerted to achieve negative permittivity properties in [35]. Although, the linear metamaterial can effectively reduce surface waves while improving main directive radiation, the basic structure of the metamaterial gives a slight matching error.

In [36] a square annular slot with four feeding lines and metasurface-based superstrate is proposed to achieve multibeam. The design met the gain and low profile requirements. The main problem with this design is that there are high-energy side lobes while performing four beams.

In this article, a hybrid metasurface using split ring resonator unit cell and U-shaped unit cell for split beam at 3.5 GHz band is presented. The antenna in this work is a microstrip patch antenna (MPA), which is used to test the proposed metasurface and test its split property.

The main purpose of splitting the beam in the proposed design compared to previous designs is to avoid the interference that comes from obstacles and buildings. In addition, the split beam technique helps in increasing the traffic capacity and reducing the size of the whole network. This leads to an increase in the efficiency of the 5G network in the urban area.

The paper is organized as follows; Section II discusses the design steps of metamaterial unit cell and metasurface array with 4×4 unit cell configuration. Section III presents the obtained results of the proposed metasurface. Finally, Section IV concludes the findings of this work.

II. METASURFACE GEOMETRY AND ANTENNA DESIGN

Generally, metasurface resonant frequency (f) is determined theoretically by its inductance (L) and capacitance (C). The resonant frequency varies by changing the values of inductance and capacitance. The resonant frequency is calculated by [25]:

$$f = 1/(2\pi(LC)^{1/2}) \tag{1}$$

Before proceeding to the main design processes, it's critical to figure out the antenna, unit cell, and metasurface design specifications. This provides a crucial indicator of how these proposed components perform at their minimum requirements. To ensure that 90 percent of the power is transmitted from port 1 of the antenna, the reflection coefficient (S_{11}) must be less than -10 dB. In this study, a gain of 5 dB or greater is sought to produce an acceptable gain value compared to an

omni-directional beam's directivity. A reflection parameter (S_{11}) of less than -10 dB is desired to ensure an adequate impedance bandwidth at the proposed frequency of 3.5 GHz. This implies the antenna is radiating at these frequencies. At the same time, a single port is activated to create a split beam. It made the pattern reconfiguration approach more understandable, which is essential for allowing the antenna to achieve many beam directions simultaneously. The performance criteria are then applied to the approach design.

Hence, metasurface is filtered by etching a lattice of elements conductivity onto a substrate dielectric which allows metasurface unit cells to configure for selected frequencies to be rejected and passed through signals. To enhance the gain of the microstrip square patch antenna and split the beam, a metasurface is designed and fabricated. Therefore, a hybrid metamaterial unit cell consists of a square split ring resonator (SSRR) and a U-shaped unit cell is proposed in this work. The whole metasurface and antenna designs use FR-4 substrate material with relative permittivity $\varepsilon_r = 4.4$, thickness $h = 1.6\,mm$, and loss tangent $\tan\delta = 0.02$.

A. DESIGN OF HYBRID METAMATERIAL UNIT CELL

The hybrid metamaterial unit cell is designed theoretically based on the SSRR and U shaped equivalent circuit as shown in Figure 1. The resonant frequency of the hybrid unit cell is obtained by [25]:

$$f_0 = (1)/(2\pi(L[(2l - g/2)C + (\varepsilon_0 wh)/2g])^{1/2}) \quad (2)$$

where g is the cut gap, l is the length of SSRR, w is the width of SSRR, h is the substrate thickness and ε_o is the permittivity in air. Hence, to calculate the capacitance and the inductance the following formulas are used [25]:

$$C = ((\varepsilon_e)^{1/2})/(c_0 Z_0) \quad (3)$$

$$L = 0.00508l\left(2.303\log_{10}(4l)/(w) - \theta\right) \quad (4)$$

$$l = (\lambda)/(N), \quad \mathrm{N} = 4, 10, 20, \ldots, \mathrm{N} - 1 \quad (5)$$

where ε_e is the effective permittivity, c_0 is the speed of light, Z_0 is the impedance of the medium, and θ is the constant based on the wire geometry. For SSRR θ is 2.853.

A parametric study on adding a single SSRR to two U shaped unit cells is performed with aid of CST software. The responses of the hybrid unit cell in terms of reflection coefficient (S_{11}) and transmission coefficient (S_{21}) are shown in Figure 2 (a) and (b) respectively.

The following equations (6)-(9) are used to extract the medium's complex permittivity (ε) and permeability (μ) from S-parameter values [37].

$$z = \pm((1 + S_{11})^2 - S_{21}^2)/((1 - S_{11})^2 - S_{21}^2))^{1/2} \quad (6)$$

$$n = \frac{1}{k_{0l}}\{[Im[ln(\exp[ink_0 l]) + 2m\pi] - iR\exp[[ln(\exp[ink_0 l])]\} \quad (7)$$

$$exp[ink_0 l] = (S_{21})/(1 - S_{11}(z - 1)/(z + 1)) \quad (8)$$

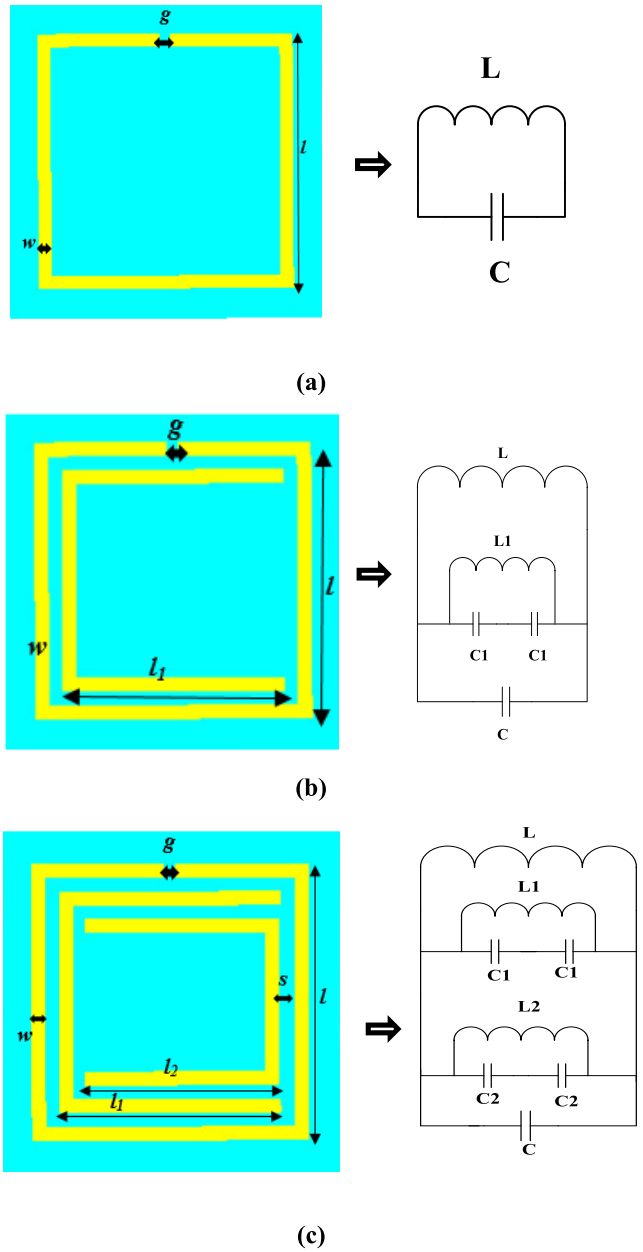

FIGURE 1. The hybrid metamaterial unit cell geometry. (a) SRR equivalent circuit. (b) SRR and U-shape equivalent circuit. (c) The proposed unit cell and the equivalent circuit.

$$\varepsilon = n/z, \quad \mu = nz \quad (9)$$

where k_0 denotes the wave number in free space, n is the refractive index, m is the integer relative to n, z is the normalize wave impedance.

The MATLAB software is used to plot the extract permittivity (ε), and permeability (μ) as shown in Figure 2 (c) and (d) respectively.

The reflection coefficient is shifted to the lower band when two U-shape unit cells are added to the SSRR unit cell as shown in Figure 2 (a). Similarly, the transmission coefficient lagging the response of the reflection coefficient as the U shape is inserted to the proposed unit cell as shown in Figure 2 (b). At the same time, the permittivity value

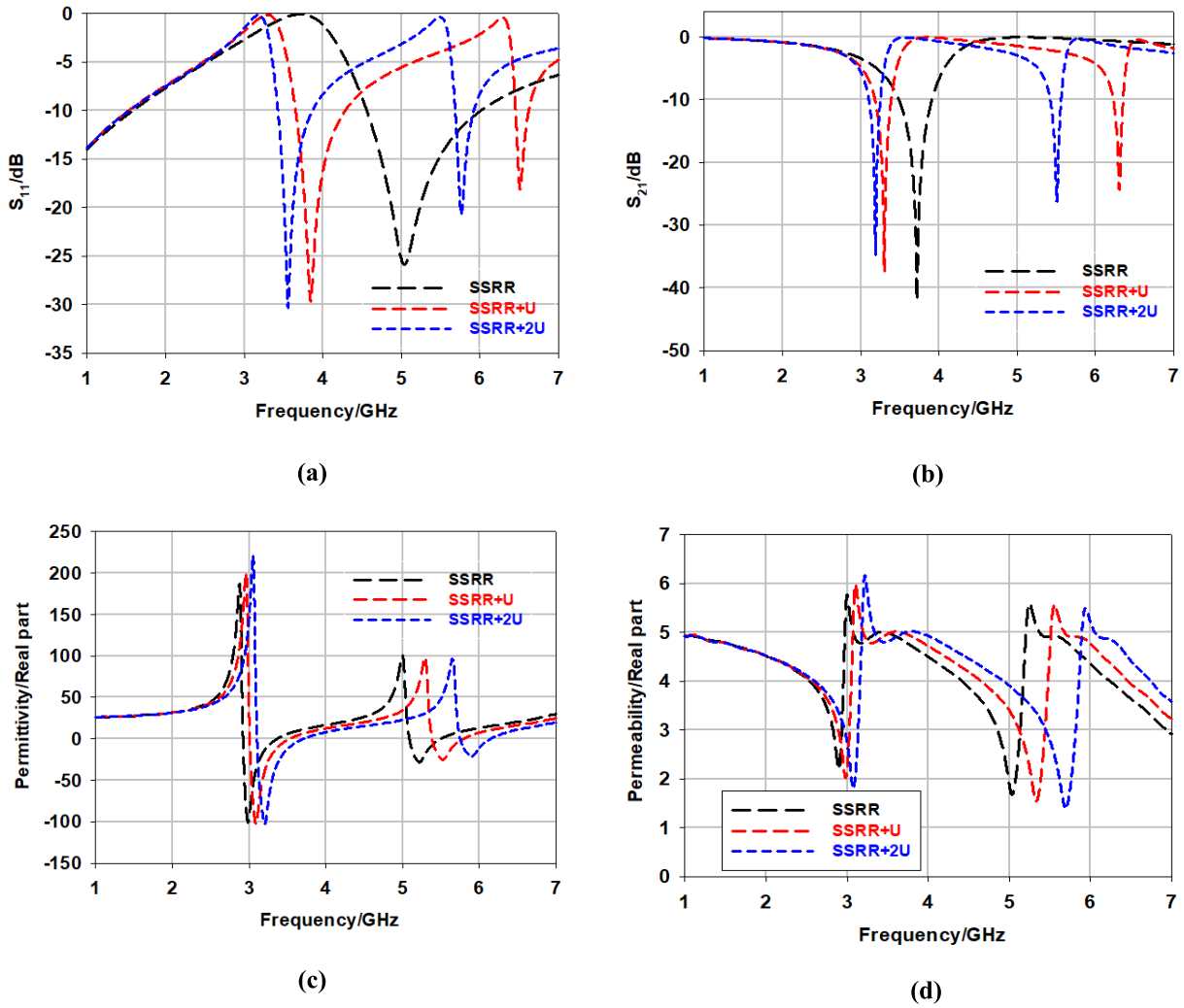

FIGURE 2. The simulated responses of the proposed unit cell. (a) Reflection coefficient. (b) Transmission coefficient. (c) Permittivity. (d) Permeability.

of the proposed unit cell is negative at the frequency range of (3 GHz to 4 GHz) with permeability staying positive at all frequency range. This gives the proposed unit cell the characteristics of epsilon-negative metamaterial (ENG) as shown in Figure 2 (c) and (d) respectively. The proposed geometry metasurface demonstrates epsilon-negative (ENG) characteristics, that restricts wave propagation and reflects all incident signals with adequate polarization. Consequently, the primary radiation gain and directivity are improved, while the antenna's back lobe radiation is reduced.

As result, Table 1 summarizes the dimensions of the proposed hybrid (SSRR+U-shaped) metamaterial unit cell at 3.5 GHz.

TABLE 1. The dimensions of the proposed SSRR+U-shape unit cell at 3.5 GHz.

Parameter	Definition	Value (mm)
L	Length of SSRR	6.5
g	Gap cut of SSRR+U-shape	0.5
w	Width of SSRR+U-shape	0.5
s	Gap between SSRR and U-shape	0.3
l1	Length of first U-shape	5.20
l2	Length of second U-shape	4.55

B. DESIGN OF 4 × 4 METASURFACE

The proposed hybrid unit cell with SSRR integrated with U shape structure to form a metasurface. The 4 × 4 metasurface structures are shown in Figure 3. Two different configurations are implemented for the proposed metasurface. The first configuration consists of unit cells arranged with the same current direction along with the four row elements. The second configuration has a unit cell distributed in opposite direction along with the two adjusted columns. This allows the current to flow oppositely inside the unit cell and split the beam into two different directions.

Metasurface compact size is sufficient for practical use to prevent wasting too much simulation time and resources.

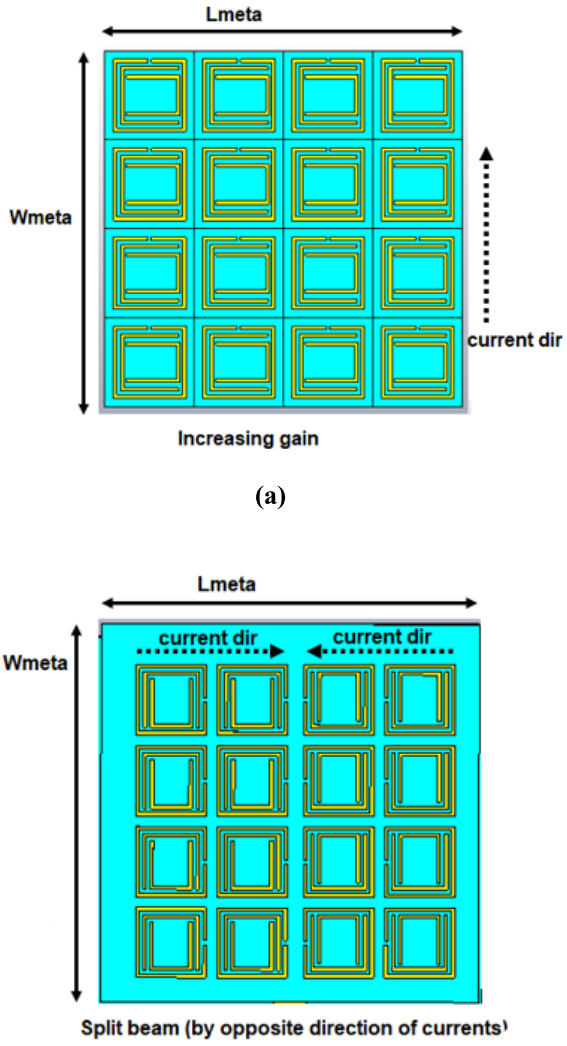

FIGURE 3. The proposed 4 × 4 metasurface configuration. (a) For increasing the gain. (b) For split beam.

For this reason, a set of 4 × 4 unit cells is chosen instead of 5 × 5 unit cells. In addition, 4 × 4 unit cells are proposed to cover the radiation element patch. Furthermore, to realize the differential-fed scheme, structural symmetry of 4 × 4 unit cells is used instead of 3 × 3 unit cells.

Full wave simulations with a time domain solver are performed using CST simulator software. The periodic boundary conditions are set in x and y directions and z direction is set to open conditions. Figure 4 presents the simulated results of the reflection coefficient, transmission coefficient, and the polarization conversion ratio (PCR). It is important to study the PCR of the proposed metasurface in order to ensure the split of the beam by opposite current flow inside the meta unit cell. PCR can be found as [38]:

$$PCR = R_{yx}^2 \Big/ \left(R_{yx}^2 + R_{xx}^2\right) \tag{10}$$

where, the co-polarization of the reflection coefficient is (R_{xx}), and (R_{yx}) is the cross-polarization of the transmission

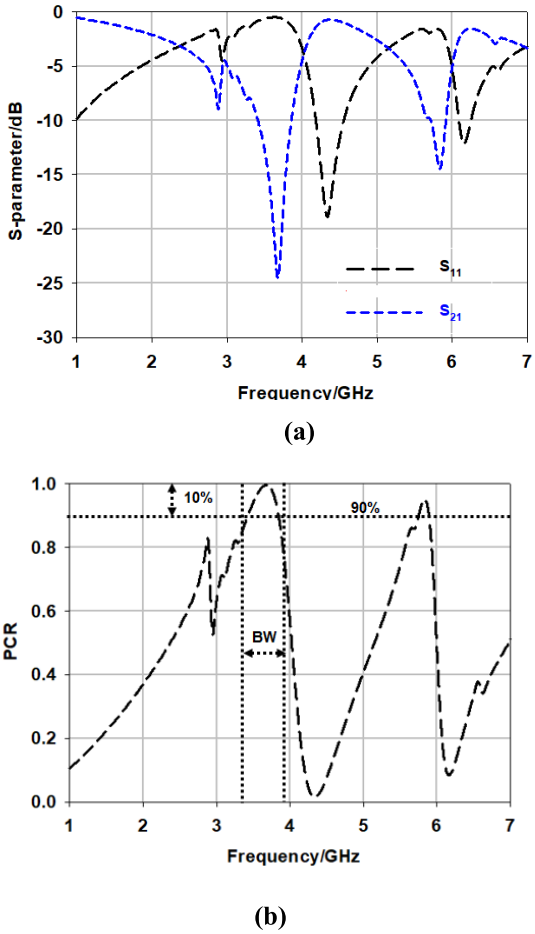

FIGURE 4. Simulated response of 4 × 4 metasurface for split beam under normal incident. (a) Reflection and transmission coefficient. (b) PCR.

coefficient. Since the metasurface structure is symmetric, PCR, co-polarization, and cross-polarization are the same under the normal x-polarized EM wave. It can be found that the co-polarization is lower than −10 dB in the frequency range from 4.17 GHz to 4.55 GHz and from 6.02 GHz to 6.22 GHz as in Figure 4(a). It can also be observed from Figure 4 (a) that there are two resonant frequencies at 4.35 GHz and 6.16 GHz respectively. The cross-polarization is higher than −1 dB as in Figure 4(a) and the metasurface transmission coefficient resonates at 3.55 GHz and 5.8 GHz under normal incidence. At those two resonant frequencies of 3.55 GHz and 5.8 GHz, the PCR values are close to 100% and higher than 90% from 3.3 GHz to 3.7 GHz and from 5.6 GHz to 5.9 GHz under normal incidence as in Figure 4 (b). Hence, the proposed metasurface demonstrates that the split beam property can be achieved.

In order to verify the effect of the proposed double-sided 4 × 4 metasurface resonators upon the single-sided 4 × 4 metasurface constructions, a parametric study to identify the electromagnetic properties of the designed metasurface in terms of reflection coefficient (S_{11}), transmission coefficient (S_{21}), effective permittivity (ε), and permeability (μ). In Figure 5 (a), the relevant return loss S_{11} responses are illustrated, at 3.28 GHz, a maximum return loss S_{11} of

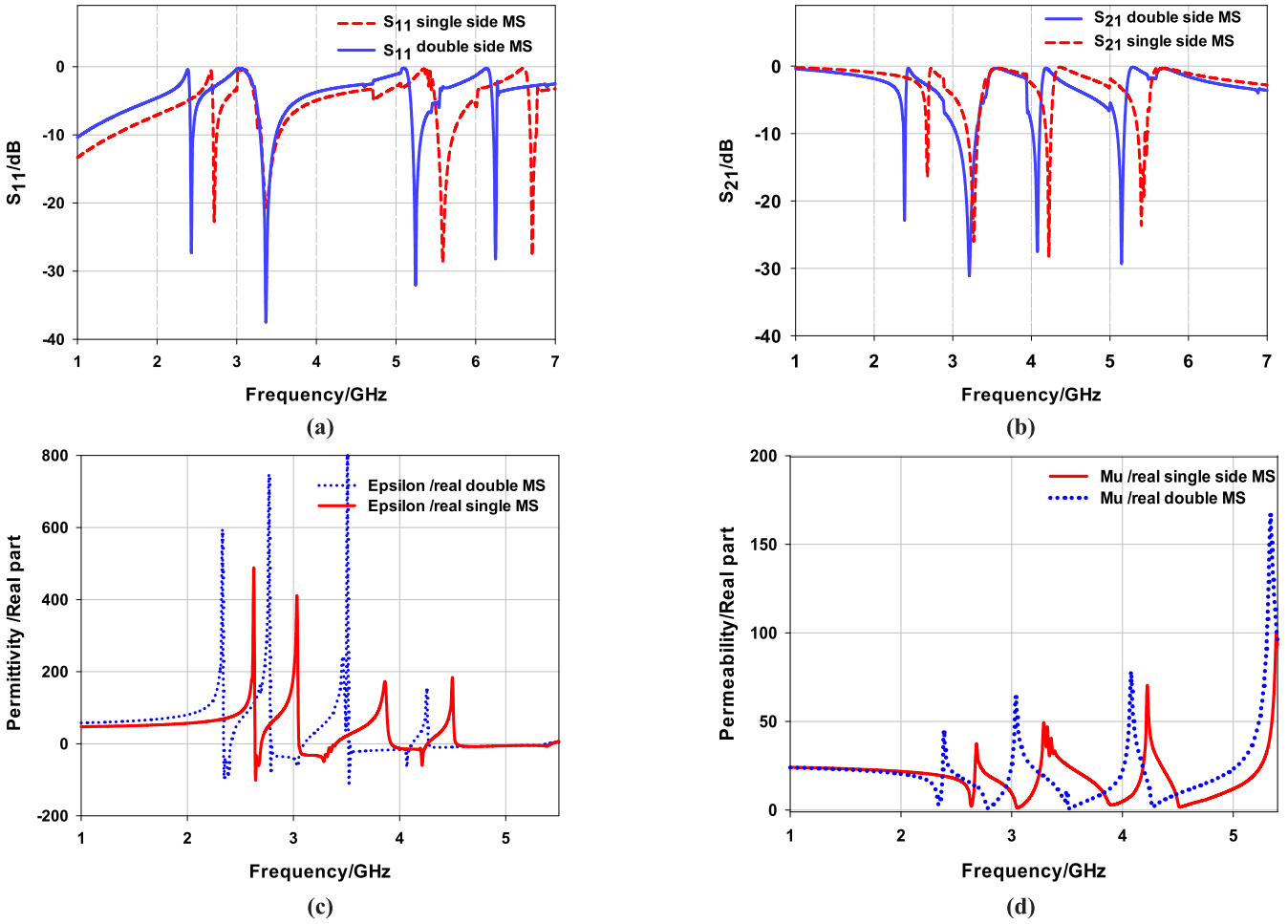

FIGURE 5. The simulated responses of the proposed metasurface for increasing the gain (single and double sided). (a) Reflection coefficient. (b) Transmission coefficient. (c) Permittivity. (d) Permeability.

−37 dB was observed without incorporating the MPA, while the S_{11} of single side configuration metasurface achieved −21 dB in the same band. In Figure 5 (b), At 3.28 GHz, a maximum transmission coefficient S_{21} of −32 dB was observed, while the S_{11} of single side configuration metasurface achieved −27 dB resonance at 3.29 GHz. From Figure 5 (c) it can be realized the real part of the effective permittivity (ε) (double sided MS) has negative band frequencies from 2.8 to 3.2 GHz, 3.5 to 4.1 GHz and 4.3 to 6 GHz. While the real part permittivity of single side MS has negative band frequencies from 3.1 to 3.4 GHz, 3.9 to 4.3 GHz and 4.6 to 6 GHz. At the same time, Figure 5 (d) illustrated that the permeability stays positive at all frequency range. This gives the proposed metasurface the characteristics of epsilon-negative metamaterial (ENG).

From Figure 5, it can be observed that in contrast to the single-sided configurations, the double-sided have mutual capacitance C and inductance L characteristics besides the effective values of self-inductance and self-capacitance. More significantly, it has been demonstrated that double-sided constructions permit to enhance the material's sensitivity to the incident EM radiation. From the metasurface construction, it can be considered the mutual capacitance surrounded by rings allows the current movements through the unit cell structure. As a result, when the total capacitance increases, the resonance frequencies shift to the lower band.

To clarify the split property, Figure 6 shows the current surface distribution of the proposed metasurface. The metasurface arrangement with the same current direction results in not splitting the beam. It increases the current flow and leads to an increase in the gain of the placed antenna as shown in Figure 6 (a). To achieve the split beam property, the unit cells are rearranged to produce opposite current flow as shown in Figure 6 (b). By observing the current flow for every two cells in one column the beam is produced in a different direction.

C. METASURFACE WITH MICROSTRIP PATCH ANTENNA

The proposed 4 × 4 metasurfaces are placed above a microstrip square patch antenna to validate the split property and increase the gain as presented in Figure 7. The MPA antenna used with metasurface is shown in Figure 7 (a), (b). Both the antenna and metasurface are implemented on FR-4 substrate with a thickness of 1.6 mm. Two layers are configured with a single patch antenna on the first layer and a superstrate layer with metasurface as the second layer is placed at a distance (d). The metasurface consists of three

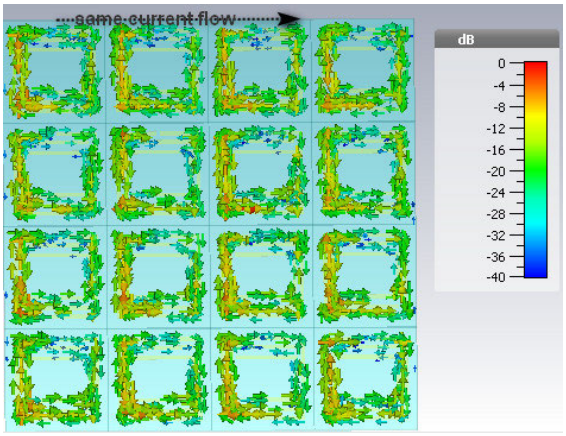

(a)

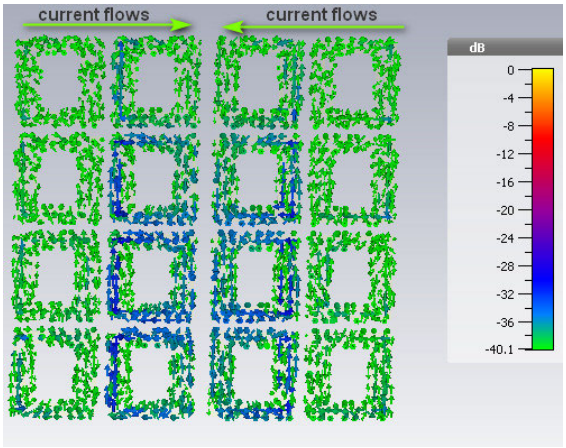

(b)

FIGURE 6. Current surface of proposed metasurface. (a) For increasing gain. (b) For splitting the beam.

layers, the first layer (bottom) is the unit cell distribution (SSRR+U shaped), the second layer is the FR-4 substrate, and the third layer (top) is a duplicated unit cell from the first layer. The distance (d) between the antenna and metasurface is air gap as in Figure 7 (c).

A parametric study based on different displacements is performed in order to achieve the optimal distance that gives a good splitting property and gain enhancement. Figure 8 (a) presents the simulated results in terms of the reflection coefficient of the antenna with respect to different d values.

At the desired frequency of 3.5 GHz, it has been found that the optimal distance is 15 mm.

At this particular distance, the antenna reflection coefficient is −25 dB with impedance bandwidth of 200 MHz compared to the MPA of −12 dB and 120 MHz impedance bandwidth. Figure 8 (b) shows that the antenna gain increases as d increases up to 15 mm. This rise in antenna gain is due to two factors: first, as the air gap widens, the electromagnetic coupling in the spacing between the two layers of the radiating patch and the metasurface widens; second, because the distance between the radiating element and the metasurface is minor in comparison to the far-field point, accordingly

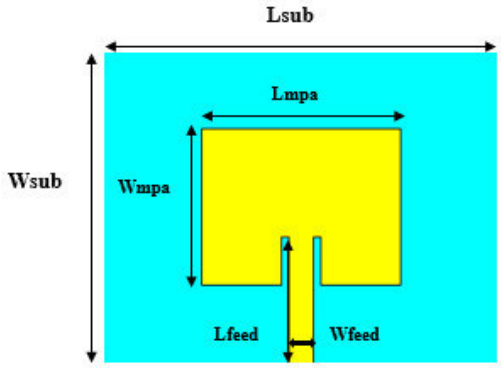

(a)

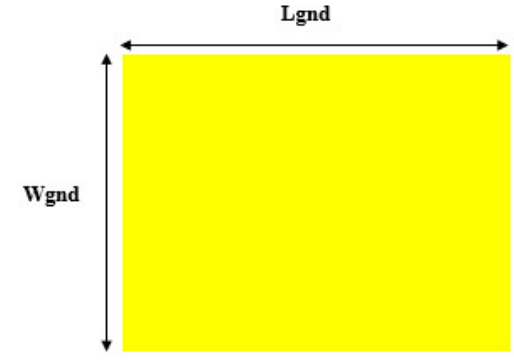

(b)

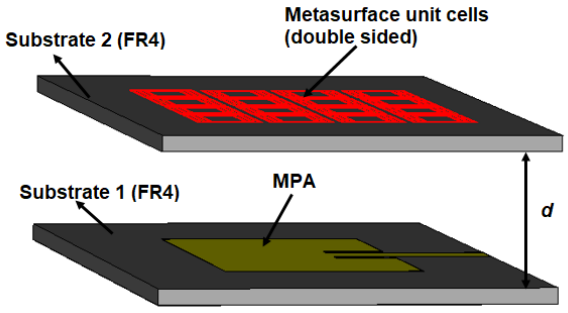

(c)

FIGURE 7. The proposed metasurface antenna configuration. (a), (b) Front and Back view of Antenna dimensions, respectively. (c) Metasurface placed above the antenna.

radiating waves of both layers are in phase, increasing the antenna's directivity. However, as the air gap rises to 20 mm, the antenna's maximum gain drops due to decreased electromagnetic coupling bounded by the top and lower radiating parts. Consider Figure 8 (c), which investigates how varying the gap d values affect the splitting performance at 3.5 GHz. The metasurface may transmit more energy when the layers separation d is narrow, and even the back lobe is considerably reduced. At the same time, the maximum split beam title is also reduced when the gap decreases at 3.5 GHz. The full-beam split title with high directivity is obtained at d = 15mm.

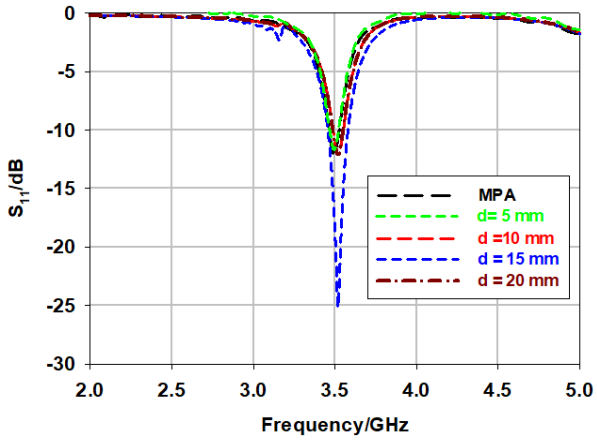

(a)

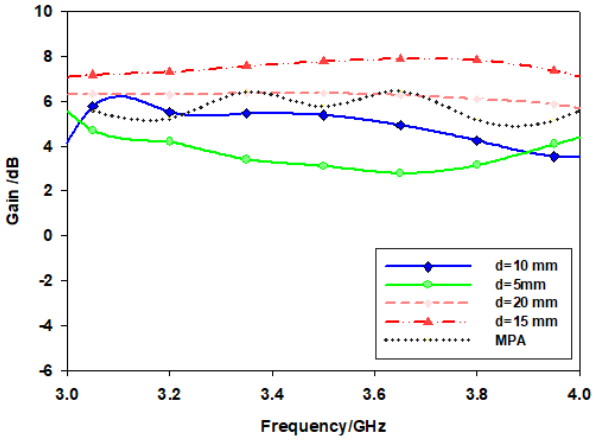

(b)

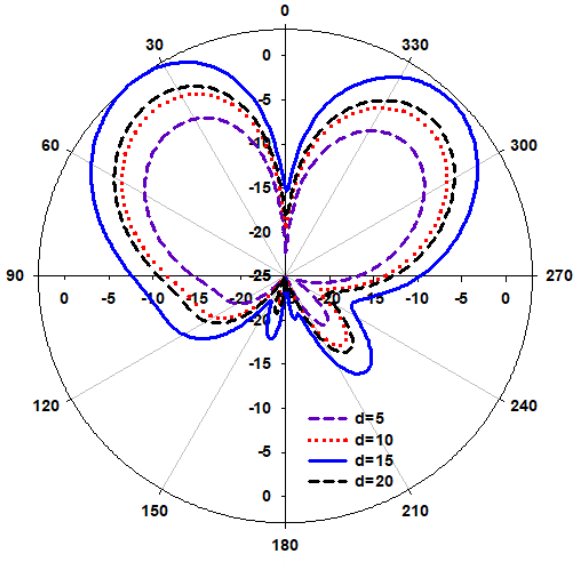

(c)

FIGURE 8. The simulated of the antenna with respect to the distance placement of the proposed metasurface in terms of: (a) reflection coefficient, (b) gain and (c) splitting beam.

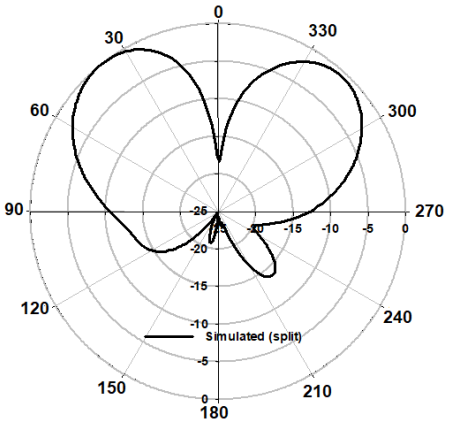

(a)

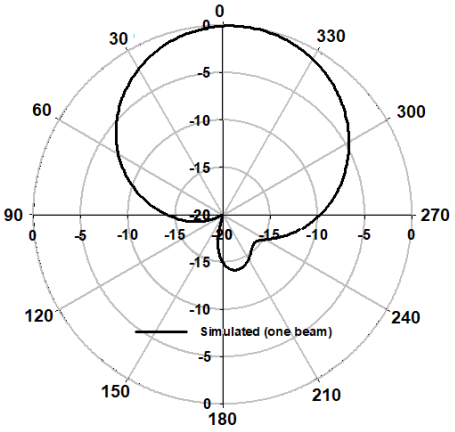

(b)

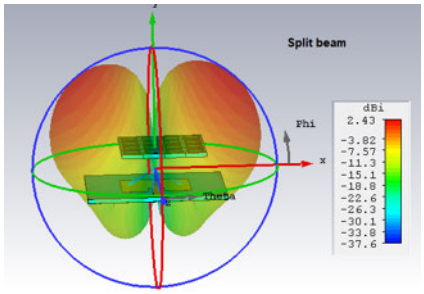

(c)

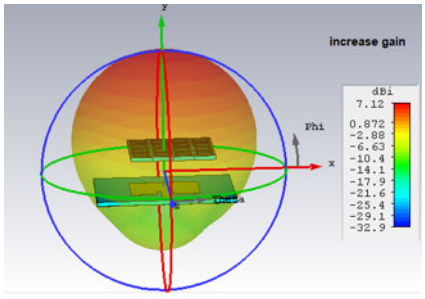

(d)

FIGURE 9. Simulated radiation pattern of the proposed metasurface with antenna. (a), (b) represent 2 D radiation pattern of two metasurface configurations (split beam and increase gain). (c), (d) 3D representation of them.

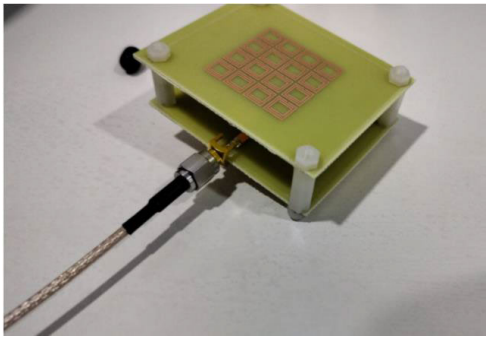

(a)

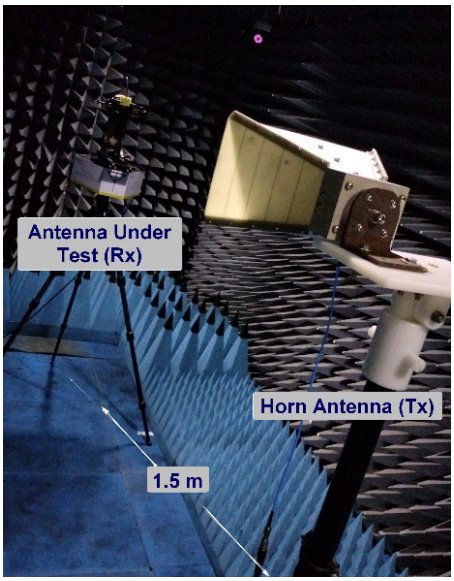

(b)

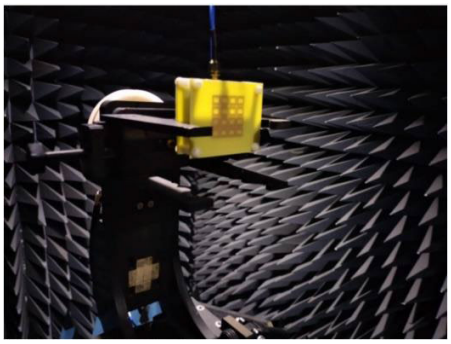

(c)

FIGURE 10. The metasurface and antenna prototype. (a) Metasurface configuration. (b) Radiation pattern measurement. (c) Antenna under test.

The co-planar and cross-planar radiation pattern is plotted at 3.5 GHz with a distance d of 15 mm as in Figure 9 (a). The directivity is increased to 7.85 dB when the proposed metasurface is applied compared to the directivity of MPA value of 4.33 dB. The beam of the antenna is split into two beams radiation pattern, which indicates that the proposed metasurface is able to split the beam correctly at ±45°. A 3D radiation pattern of the antenna is presented in Figure 9 (c) which clearly shows the split property of the beam by the proposed metasurface. The dimensions of the proposed antenna and metasurface are summarized in Table 2.

TABLE 2. The dimensions of the 4 × 4 metasurface with antenna at 3.5 GHz.

Parameter	Definition	Value (mm)
Lsub	Substrate length	52.62
Wsub	Substrate width	40.40
Lmeta	Metasurface length	52.62
Wmeta	Metasurface width	40.40
Lgnd	Ground length	52.62
Wgnd	Ground width	40.40
Lmpa	Patch length	26.31
Wmpa	Patch width	20.20
Lfeed	Feed length	15.25
Wfeed	Feed length	3.127
d	Air gap distance	15

TABLE 3. The simulation result with the measured result of the suggested antenna are compared in their performance.

Results	Simulated	Measured
S11 (dB)	-25	-15
Max. Gain achieved (dB)	7.21	6.74
Bandwidth (MHz)	200	185
Radiation Efficiency	84%	82%

III. RESULTS AND DISCUSSION

In this section, the fabricated metasurface with antenna and its measurement results are presented. The fabricated prototype and the measurement setup are shown in Figure 10. The 4 × 4 metasurface is placed over the patch antenna at an optimum height of 15 mm as in Figure 10 (a). Then, the tested prototype is placed in front of the source horn antenna surrounded by absorbing materials. The test prototype is fixed on two vertical arms of a rotating stand as in Figure 10 (b), (c). The distance between the transmitter and receiver is set to be 1.5 m, which is in far field region based on the diameter of the antenna substrate.

Figure 11 illustrates the simulated and measured results of the metasurface antenna in terms of reflection coefficient and radiation pattern. The measured results are in good agreement with the simulated predictions. The measured reflection coefficient of −15 dB is obtained at 3.5 GHz as shown in Figure 11 (a). However, a 10 dB loss difference between the measured and simulated reflection is observed. This could be referred to as the mismatch alignment of the connector port,

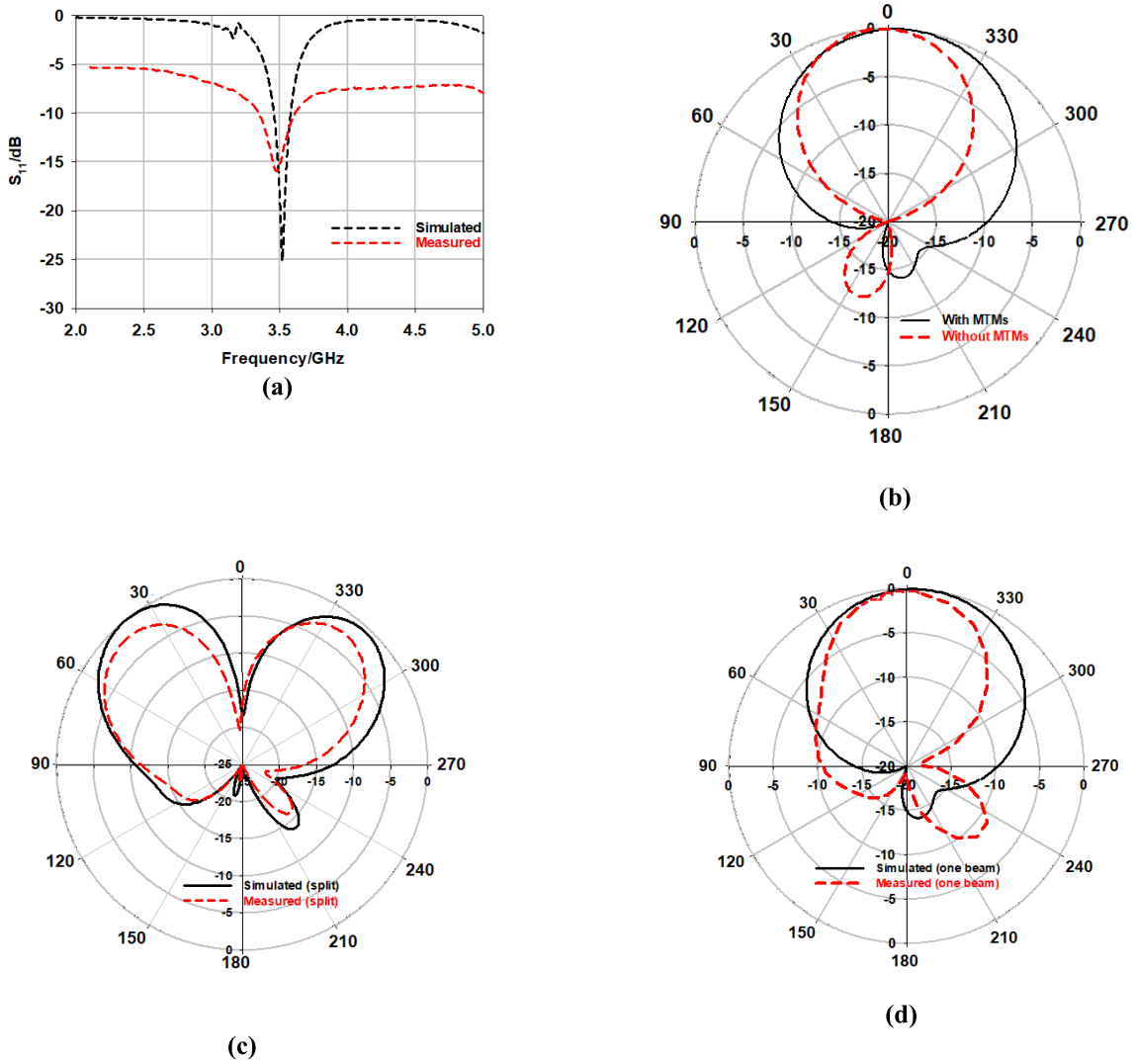

FIGURE 11. Measured results of the proposed metasurface with antenna. (a) Reflection coefficient. (b) Radiation pattern of MPA with and without MTMs. (c) Radiation pattern of split beam. (d) Radiation pattern of increasing gain.

in addition to the cable loss after calibration which is noticed to be 5 dB.

In Figure 11 (b), the radiation patterns of the MPA with and without metasurface are measured to verify the gain improvement of the proposed antenna. It is also observed the narrow gain is enhanced to 7.21 dB, while measured realized gain is 6.74 dB as shown in Figure 11 (d).

Two broadside beams of gain 2.65 dB within reduction in half-power beamwidth (HPBW) are observed as in Figure 11 (c). The E-plane of the antenna has a split beam by the designed metasurface.

The realized gains of the simulated and measured results are almost a match. These close results have been detected in view of the presence of a metasurface on a basic conventional patch. Furthermore, the shift could be caused by SMA connector insertion loss.

The analysis and simulation in Figure 11 (b), (c) and (d) indicate that bare MPA has a radiation efficiency of 78% with main lobe direction toward 7.0°, 3 dB beam width is 102.3°, and side lobe level has been considered −12.9 dB. Meanwhile, the MPA with superstrate metasurface configuration for increasing the gain has a radiation efficiency of 84%, 3 dB beam width is 77.5°, and the main lobe is directed normalize towards 0° with a side lobe level −14.9 dB at the resonant frequency. Besides, compared to other proposed antennas provided in [39]–[42], it has acceptable radiation efficiency, bandwidth, and gain. Furthermore, the radiation efficiency is more than 82% of MPA with superstrate metasurface configuration for splitting the beam, 3 dB beam width is 52.7 °, and a side lobe level of −11 dB at the resonant frequency. Hence, it is observed that the insertion of a metasurface to a simple conventional patch improves its performance in terms of radiation efficiency, 3 dB beam width and main lobe direction. The decrease in the 3 dB beam width value indicates a more directive beam and gain enhancement.

Relative to the field coupling, the patch feed's surface current distribution will be altered, and currents will be motivated on the metasurface. Consequently, the patch

TABLE 4. Comparison of the proposed design with several high-performance recent works.

Ref.	f_0 (GHz)	Band (GHz)	Antenna type	No.of source antenna	Unit cell type / No. Unit cell in array	Overall system dimensions $(\lambda_0)^3$	d (mm)	Technique employed	Aim	Beam split	Beam tilt
22	5	(4.95-5.1)	Rectangular aperture	One	SRR / 12 × 12	4×4×0.0255	10	MS as superstrate	Beamwidth control	One	0°
23	2.5	(2.4-2.5)	Slot-fed	One	Closed square ring / 5×5	0.96×0.96×0.07	8.5	MS as superstrate	Beam steering	One	±35°
27	10	(9.6-10)	Rectangular waveguide-fed	Feed layer	Nyquist/8×12	7.64×4×0.0254	----	Constructed for hollow waveguides	Beam steering	One	±15°
28	5.3	(5.24-5.34)	Fabry-Perot-cavity	One	MCRR/5×5	1.24×1.24×0.0134	30	MS as superstrate	High gain	One	0°
30	5.2	(5.2-5.5)	monopole antenna	One	3 layers of FSS/8×4/8×4/4×4	0.8×0.8×1.6	96	Dual layers are set to be vertical to the antenna and one layer on the top	Beam reconfigurable	dual-beam	±90°
32	2.45	(2.4-2.5)	Dipole excitation	One	Double SRR with PIN diodes /3×3	0.655×0.655×0.018	10	MS as superstrate	Beam switching	One	0° 180°
33	12	(11.6-12.2)	SIW	two	Programmable PIN diodes/16	4.8 × 0.64 × 0.0254	---	Built-in with hollow waveguides	Beam switching	dual-beam for code 7	+30° -25°
35	5	(4.89-5.12)	MPA	One	five loops of metal wire (ENG type)	1.918 × 1.918×0.033	---	surrounding the patch	Directivity	One	0°
36	5	4.9–5.05	Square annular slot with 4 feeding lines	Four ports excited	multi-size metal square /2 layers (5×5)	1.08×1.08×0.08	0.9	MS as superstrate	High gain	One o/p beam for each i/p port	32°
This work	3.5	(3.4-3.6)	MPA	One	SSRR+dual U-shape/4×4	0.61×0.45×0.018	15	MS as superstrate	Beam split	Two split beams	±45°

antenna serves as the primary MPA feeder, while the metasurface is the central aperture for radiating energy into the free space. As a result of the feed-to-aperture coupling, the phase correction antenna can be changed to have a wider matching bandwidth of 200 MHz than the bandwidth of MPA without metasurface is 120MHz.

TABLE 3 presents the performance analysis of simulated and experimental outcomes for the proposed antenna.

In summary, Table 4 compares the performance of the previously reported beam-steering antennas using metasurface to the proposed work, in terms of antenna type, bands (GHz), overall system dimensions, unit cell type, number of the unit cells in the array, the separation distance between antenna and metasurface layer, the metasurface technique employed, the main purpose of each design, gain enhancement achieve, number of beams split and scanning angle. Although a linear comparison is unattainable because they are all different and have varying numbers of elements, it is reasonable to conclude that the metasurface suggested in this paper has the highest scanning angle while maintaining a compact structure, upgrading metasurface will not be complex as in [31]–[34].

The critical considerations in this design approach are to realize the gain, antenna size, reduced power consumption and cost of sectors with split beams. It is vital to emphasize that the proposed technique offers a preference upon typical active tuning approaches in [32] and [33], which demand vast quantities of diodes, biasing circuits for alterable or reconstructed metasurface. Besides, it is considered in recent works [43], [44] that increasing elements on multi-beam antenna such as massive MIMO antenna arrays for 5G technology will increase the losses between mutual coupling elements. Moreover, as compared to large metamaterials or typical metasurfaces, less-layer metasurfaces might allow more flexibility to alter electromagnetic waves, neither sacrificing efficiency nor increasing fabrication complexity. Nowadays, metasurface for polarization phase modification of electromagnetic waves significantly affects real-world applications as the metasurface fabrication technology improves. This metasurface design contributes a novel directional in 5G communication technique, which is required to achieve multiple beam directions simultaneously.

The split beam is produced by activating a single port. It simplifies comprehension of the pattern reconfiguration

technique, which is significant in 5G Pico cell base station at 3.5GHz.

Overall, the metasurface splits the main beam from MPA into two equal beams successfully at ±45°.

IV. CONCLUSION

The design of a hybrid metasurface based on SSRR and U-shaped unit cells for split the antenna beam is successfully designed and fabricated. The metasurface prototype is measured after being placed over a microstrip patch antenna at 3.5 GHz. The measurement reflection coefficient agrees well with the simulated one, the reflection coefficient less than −10 dB at the desired frequency. A gain enhancement of 3.5 dB is obtained at the broad side of the direction of the antenna at the required impedance bandwidth. A split beam is successfully observed in the E-plane with 2.65 dB gain for each beam. The split direction has two beam tilt angles at −45° and 45° respectively. This metasurface type can be used for beam steering technology required in 5G mobile applications at 3.5 GHz Pico cell.

REFERENCES

[1] M. F. Imani, J. N. Gollub, O. Yurduseven, A. V. Diebold, M. Boyarsky, T. Fromenteze, L. Pulido-Mancera, T. Sleasman, and D. R. Smith, "Review of metasurface antennas for computational microwave imaging," *IEEE Trans. Antennas Propag.*, vol. 68, no. 3, pp. 1860–1875, Mar. 2020.

[2] M. Faenzi, G. Minatti, D. González-Ovejero, F. Caminita, E. Martini, C. D. Giovampaola, and S. Maci, "Metasurface antennas: New models, applications and realizations," *Sci. Rep.*, vol. 9, no. 1, pp. 1–14, Dec. 2019.

[3] X. Tong, Z. H. Jiang, C. Yu, F. Wu, X. Xu, and W. Hong, "Low-profile, broadband, dual-linearly polarized, and wide-angle millimeter-wave antenna arrays for *ka*-band 5G applications," *IEEE Antennas Wireless Propag. Lett.*, vol. 20, no. 10, pp. 2038–2042, Oct. 2021.

[4] I.-J. Nam, S. Lee, and D. Kim, "Miniaturized beam reconfigurable reflectarray antenna with wide three-dimensional beam coverage," *IEEE Trans. Antennas Propag.*, early access, Jun. 2, 2021, doi: 10.1109/TAP.2021.3083732.

[5] S. J. Yang, Y. Yang, and X. Y. Zhang, "Low scattering element-based aperture-shared array for multiband base stations," *IEEE Trans. Antennas Propag.*, vol. 69, no. 12, pp. 8315–8324, Dec. 2021.

[6] M. Abdullah, A. Altaf, M. R. Anjum, Z. A. Arain, A. A. Jamali, M. Alibakhshikenari, F. Falcone, and E. Limiti, "Future smartphone: MIMO antenna system for 5G mobile terminals," *IEEE Access*, vol. 9, pp. 91593–91603, 2021.

[7] S. Li, Z. N. Chen, T. Li, F. H. Lin, and X. Yin, "Characterization of metasurface lens antenna for sub-6 GHz dual-polarization full-dimension massive MIMO and multibeam systems," *IEEE Trans. Antennas Propag.*, vol. 68, no. 3, pp. 1366–1377, Mar. 2020.

[8] C. Milias, R. B. Andersen, P. I. Lazaridis, Z. D. Zaharis, B. Muhammad, J. T. B. Kristensen, A. Mihovska, and D. D. S. Hermansen, "Metamaterial-inspired antennas: A review of the state of the art and future design challenges," *IEEE Access*, vol. 9, pp. 89846–89865, 2021.

[9] A. Pander, H. Hamada, and H. Nosaka, "Excitation of resonances in planar metamaterials at a two-layer dielectric interface for substrate integrated electronics," *Phys. Lett. A*, vol. 409, Sep. 2021, Art. no. 127523.

[10] T. Hayat, M. U. Afzal, A. Lalbakhsh, and K. P. Esselle, "Additively manufactured perforated superstrate to improve directive radiation characteristics of electromagnetic source," *IEEE Access*, vol. 7, pp. 153445–153452, 2019.

[11] J. J. de Oliveira, L. D. Ribeiro, E. J. da Silva, and R. M. de Souza Batalha, "Design of a free space metamaterial lens based on LC parameters at S-band," *J. Electromagn. Waves Appl.*, vol. 35, no. 16, pp. 1–14, Jun. 2021.

[12] S. Abdullah, G. Xiao, and R. E. Amaya, "A review on the history and current literature of metamaterials and its applications to antennas & radio frequency identification (RFID) devices," *IEEE J. Radio Freq. Identificat.*, vol. 5, no. 4, pp. 427–445, Dec. 2021.

[13] S. L. Madsen and J. S. Bobowski, "The complex permeability of split-ring resonator arrays measured at microwave frequencies," *IEEE Trans. Microw. Theory Techn.*, vol. 68, no. 8, pp. 3547–3557, Aug. 2020.

[14] S. Sithara and Z. N. Chen, "Low-profile broadband dual-polarization dou-ble-layer metasurface antenna for 2G/3G/LTE cellular base-stations," *IEEE Trans. Antennas Propag.*, early access, Jul. 26, 2021, doi: 10.1109/TAP.2021.3098554.

[15] L. Bao, R. Y. Wu, X. Fu, Q. Ma, G. D. Bai, J. Mu, R. Jiang, and T. J. Cui, "Multi-beam forming and controls by metasurface with phase and amplitude modulations," *IEEE Trans. Antennas Propag.*, vol. 67, no. 10, pp. 6680–6685, Oct. 2019.

[16] A. Lalbakhsh, M. U. Afzal, T. Hayat, K. P. Esselle, and K. Mandal, "All-metal wideband metasurface for near-field transformation of medium-to-high gain electromagnetic sources," *Sci. Rep.*, vol. 11, no. 1, pp. 1–9, Dec. 2021.

[17] M. U. Afzal, L. Matekovits, K. P. Esselle, and A. Lalbakhsh, "Beam-scanning antenna based on near-electric field phase transformation and refraction of electromagnetic wave through dielectric structures," *IEEE Access*, vol. 8, pp. 199242–199253, 2020.

[18] S. Adibi, M. A. Honarvar, and A. Lalbakhsh, "Gain enhancement of wide-band circularly polarized UWB antenna using FSS," *Radio Sci.*, vol. 56, no. 1, pp. 1–8, Jan. 2021.

[19] X. Chen, H. Zou, M. Su, L. Tang, C. Wang, S. Chen, C. Su, and Y. Li, "All-dielectric metasurface-based beam splitter with arbitrary splitting ratio," *Nanomaterials*, vol. 11, no. 5, p. 1137, Apr. 2021.

[20] M. Ameen, A. Mishra, and R. K. Chaudhary, "Dual-band CRLH-TL inspired antenna loaded with metasurface for airborne applications," *Microw. Opt. Technol. Lett.*, vol. 63, no. 4, pp. 1249–1256, Apr. 2021.

[21] J. Park, M. Jeong, N. Hussain, S. Rhee, S. Park, and N. Kim, "A low-profile high-gain filtering antenna for fifth generation systems based on nonuniform metasurface," *Microw. Opt. Technol. Lett.*, vol. 61, no. 11, pp. 2513–2519, Nov. 2019.

[22] J. Xiong, Y. Hu, S. Mao, W. Zhang, S. Xiao, and B.-Z. Wang, "Agile beamwidth control and directivity enhancement for aperture radiation with low-profile metasurfaces," *IEEE Trans. Antennas Propag.*, vol. 66, no. 3, pp. 1528–1533, Mar. 2018.

[23] T. Hongnara, S. Chaimool, P. Akkaraekthalin, and Y. Zhao, "Design of compact beam-steering antennas using a metasurface formed by uniform square rings," *IEEE Access*, vol. 6, pp. 9420–9429, 2018.

[24] Y. He, B.-X. Wang, P. Lou, and H. Zhu, "Multiple-band absorber enabled by new type of metamaterial resonator formed by metallic split ring embedded with rectangle patch," *Results Phys.*, vol. 18, Sep. 2020, Art. no. 103251.

[25] J. C. Tie, D. R. Smith, and L. Ruopeng, *Metamaterials Theory, Design, and Applications*. New York, NY, USA: Springer, 2010.

[26] K. Sakoda, *Electromagnetic Metamaterials: Modern Insights into Macroscopic Electromagnetic Fields*, vol. 287. Tsukuba, Japan: National Institute for Materials Science, 2019.

[27] M. Boyarsky, T. Sleasman, M. F. Imani, J. N. Gollub, and D. R. Smith, "Electronically steered metasurface antenna," *Sci. Rep.*, vol. 11, no. 1, pp. 1–10, Dec. 2021.

[28] A. K. Singh, M. P. Abegaonkar, and S. K. Koul, "Wide gain enhanced band high gain Fabry–Pérot cavity antenna using ultrathin reflecting metasurface," *Microw. Opt. Technol. Lett.*, vol. 61, no. 6, pp. 1628–1633, Jun. 2019.

[29] Z. Zhang, W. Zhang, Y. Liu, R. Ma, R. Yang, and L. Han, "Two-dimensional broadband and wide angle scanning multi-beam antenna based on leaky-wave metasurface," *Int. J. RF Microw. Comput.-Aided Eng.*, vol. 32, no. 1, p. e22922, Jan. 2022.

[30] P. Das, K. Mandal, and A. Lalbakhsh, "Single-layer polarization-insensitive frequency selective surface for beam reconfigurability of monopole antennas," *J. Electromagn. Waves Appl.*, vol. 34, no. 1, pp. 86–102, Nov. 2019.

[31] K. K. Katare, S. Chandravanshi, A. Biswas, and M. J. Akhtar, "Realization of split beam antenna using transmission-type coding metasurface and planar lens," *IEEE Trans. Antennas Propag.*, vol. 67, no. 4, pp. 2074–2084, Apr. 2019.

[32] S. Chaimool, T. Hongnara, C. Rakluea, P. Akkaraekthalin, and Y. Zhao, "Design of a PIN diode-based reconfigurable metasurface antenna for beam switching applications," *Int. J. Antennas Propag.*, vol. 2019, pp. 1–7, Jan. 2019.

[33] S. Li, F. Xu, X. Wan, T. J. Cui, and Y.-Q. Jin, "Programmable metasurface based on substrate-integrated waveguide for compact dynamic-pattern antenna," *IEEE Trans. Antennas Propag.*, vol. 69, no. 5, pp. 2958–2962, May 2021.

[34] W. Li, T. Qiu, J. Wang, L. Zheng, Y. Jing, Y. Jia, H. Wang, Y. Han, and S. Qu, "Programmable coding metasurface reflector for reconfigurable multibeam antenna application," *IEEE Trans. Antennas Propag.*, vol. 69, no. 1, pp. 296–301, Jan. 2021.
[35] W.-H. Hui, Y. Guo, and X.-P. Zhao, "A simple linear-type negative permittivity metamaterials substrate microstrip patch antenna," *Materials*, vol. 14, no. 16, p. 4398, Aug. 2021.
[36] Z. Zhao and W. Zhang, "Multi-beam antenna based on annular slot and uneven metasurface," *Int. J. RF Microw. Comput.-Aided Eng.*, vol. 31, no. 11, p. e22814, Nov. 2021.
[37] S. Datta, S. Mukherjee, X. Shi, M. Haq, Y. Deng, L. Udpa, and E. Rothwell, "Negative index metamaterial lens for subwavelength microwave detection," *Sensors*, vol. 21, no. 14, p. 4782, Jul. 2021.
[38] F. Ahmed, M. I. Khan, and F. A. Tahir, "A multi-functional polarization transforming metasurface for *C*, *X* and *K* band applications," *IEEE Antennas Wireless Propag. Lett.*, vol. 20, no. 11, pp. 2186–2190, Mar. 12, 2021.
[39] H.-T. Zhong, X.-X. Yang, C. Tan, and K. Yu, "Triple-band polarization-insensitive and wide-angle metamaterial array for electromagnetic energy harvesting," *Appl. Phys. Lett.*, vol. 109, no. 25, Dec. 2016, Art. no. 253904.
[40] G. T. O. Tékam, V. Ginis, J. Danckaert, and P. Tassin, "Designing an efficient rectifying cut-wire metasurface for electromagnetic energy harvesting," *Appl. Phys. Lett.*, vol. 110, no. 8, Feb. 2017, Art. no. 083901.
[41] X. Zhang, H. Liu, and L. Li, "Tri-band miniaturized wide-angle and polarization-insensitive metasurface for ambient energy harvesting," *Appl. Phys. Lett.*, vol. 111, no. 7, Aug. 2017, Art. no. 071902.
[42] M. Khanjarian, M. Soleimani, V. Nayyeri, M. E. Badawe, S.-F. Babazadeh, and O. M. Ramahi, "A circularly polarized, high aperture efficiency meta- surface antenna," *Microw. Opt. Technol. Lett.*, vol. 63, no. 12, pp. 3027–3034, 2021.
[43] S. Zhang, X. Chen, and G. F. Pedersen, "Mutual coupling suppression with decoupling ground for massive MIMO antenna arrays," *IEEE Trans. Veh. Technol.*, vol. 68, no. 8, pp. 7273–7282, Aug. 2019.
[44] F. A. Dicandia and S. Genovesi, "Spectral efficiency improvement of 5G massive MIMO systems for high-altitude platform stations by using triangular lattice arrays," *Sensors*, vol. 21, no. 9, p. 3202, May 2021.

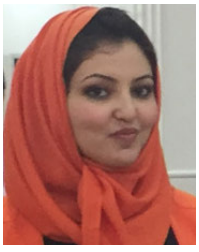

TAMARA Z. FADHIL received the B.Sc. and M.Sc. degrees from the Electrical and Electronic Engineering Department, University of Technology, Baghdad, Iraq. She is currently pursuing the Ph.D. degree in electrical engineering with Universiti Teknologi Malaysia. From 2015 to 2017, she was an Assistant Lecturer with the College of Engineering, Al-Iraqia University, Iraq. She has been a Lecturer with the University of Information Technology and Communications (UOITC), Baghdad, since December 2016, where she was a member of the Smart Cities Division, in 2018. She has several contributions in pertinent journals and conference publications. She received many honors, awards, and certificate from these universities, ITEC Program, and Knauf Germany Systems. For non-academic experience, she worked as an Electrical Engineer with the Ministry of Municipalities and Public Work, from 2010 to 2012. In 2018, she was a Leader of several successful positions, such as the Head of the Student Activities Division, Faculty of Engineering, UOITC, and the Engineering College Council Coordinator, UOITC. Besides, she was a member of the Examination Committee with UOITC, in 2017 and 2018. Her current research interest includes the design of multiple beam metasurface antenna systems for fifth-generation applications. She has participated in the IEEE 2018 International Conference on Advanced Science and Engineering (ICOASE).

NOOR ASNIZA MURAD (Senior Member, IEEE) received the B.E. degree in electrical and telecommunications engineering and the M.E. degree in electrical engineering from Universiti Teknologi Malaysia (UTM), in 2001 and 2003, respectively, and the Ph.D. degree from the Emerging Device Technology Group, University of Birmingham, U.K., in 2011, for research on micromachined millimeterwave circuits. Shortly after graduation, she served UTM as a Tutor with the Department of Radio Communication Engineering (RaCED), Faculty of Electrical Engineering (FKE), UTM, where she was appointed as a Lecturer, in April 2003. She is currently an MBOT Professional Technologist and an Associate Professor with the School of Electrical Engineering, UTM. She attached to HID GLOBAL Sdn Bhd, for one year, under research and development specifically working on RFID tag design, testing, and development. Her research interests include antenna design for RF and microwave communication systems, millimeterwave circuits design, RFID, and antenna beamforming.

MOHAMAD KAMAL A. RAHIM (Senior Member, IEEE) was born in Alor Setar, Malaysia, in 1964. He received the B.Eng. degree in electrical and electronic engineering from the University of Strathclyde, U.K., in 1987, the master's degree in engineering from the University of New South Wales, Australia, in 1992, and the Ph.D. degree in wideband active antenna from the University of Birmingham, U.K., in 2003. From 1992 to 1999, he was a Lecturer with the Faculty of Electrical Engineering, Universiti Teknologi Malaysia, where he was a Senior Lecturer with the Department of Communication Engineering, from 2005 to 2007, and is currently a Professor. His research interests include the design of active and passive antennas, dielectric resonator antennas, microstrip antennas, reflectarray antennas, electromagnetic bandgap, artificial magnetic conductors, left-handed metamaterials, and computer-aided design for antennas.

M. R. HAMID received the M.Sc. degree in communication engineering from Universiti Teknologi Malaysia (UTM), Johor Bahru, Malaysia, in 2001, and the Ph.D. degree from the University of Birmingham, Birmingham, U.K., in 2011. He has been with the Faculty of Electrical Engineering (FKE), UTM, since 1999, where he is currently a Senior Lecturer. His major research interest includes reconfigurable antenna design for multimode wireless applications.

LEVY OLIVIA NUR (Member, IEEE) received the B.E., M.E., and Ph.D. degrees in electrical engineering, majoring in telecommunication engineering from Institut Teknologi Bandung, Indonesia, in 2001, 2004, and 2014, respectively. From 2002 to 2003, during her study in master's program, she joined the Japanese University Studies in Science Technology (JUSST), as a Visiting Student with The University of Electro-Communications (UEC), Tokyo, Japan. She joined Telkom University (previously known as Institut Teknologi Telkom, ITTelkom), Bandung, Indonesia, as a Lecturer, in 2010. Her research interests include microwave absorbent material, wearable antenna, and its characterization.